



ELSEVIER

Available online at [www.sciencedirect.com](http://www.sciencedirect.com)

ScienceDirect

journal homepage: [www.elsevier.com/locate/ijrefrig](http://www.elsevier.com/locate/ijrefrig)

# Fault diagnosis of a vapor compression refrigeration system with hermetic reciprocating compressor based on p-h diagram

Necati Kocyigit <sup>a,\*</sup>, Huseyin Bulgurcu <sup>b</sup>, Cheng-Xian Lin <sup>c</sup>

<sup>a</sup> Dept. of Energy Systems Eng., Faculty of Engineering, Recep Tayyip Erdogan Univ., Rize, Turkey

<sup>b</sup> Dept. of Mech. Eng., Faculty of Eng. and Architecture, Balikesir Univ., Balikesir, Turkey

<sup>c</sup> Dept. of Mech. and Mater. Eng., Florida International Univ., Miami, FL, USA

## ARTICLE INFO

### Article history:

Received 19 January 2014

Received in revised form

16 May 2014

Accepted 31 May 2014

Available online 11 June 2014

### Keywords:

Vapor refrigeration

Fault diagnosis

p-h diagram

Thermodynamic cycle

## ABSTRACT

The aim of this study is to show how to use the p-h diagram successfully for diagnosing faults in the vapor compression refrigeration cycle. This new approach is able to remove the gap between the information required to apply a general theory of diagnosis and the limited information on the p-h diagram. With this approach, an expert may interpret more failures of the refrigeration systems. In this study, an experimental setup with eight artificial faults was used to demonstrate the implementation of diagnosis. It is approved that with the assistant of cycles on the p-h diagrams, the difference between normal and faulty conditions can be easily observed.

© 2014 Elsevier Ltd and IIR. All rights reserved.

## Diagnostic d'erreurs d'un système frigorifique à compression de vapeur avec un compresseur à piston hermétique basé sur un diagramme p-h

Mots clés : Froid par évaporation ; Diagnostic d'erreurs ; Diagramme p-h ; Cycle thermodynamique

### 1. Introduction

It is well known that performance degradation resulting from the development of faults within vapor compression systems can result in significant increases in energy consumption

(McIntosh et al., 2000). Since cooling and refrigeration compromise over a third of the electrical energy consumption in residential and commercial buildings, the development of diagnostic modules that can effectively detect incipient faults could result in significant cost and energy savings that would have a dramatic economic and environmental impact.

\* Corresponding author. Tel.: +90 5308823740; fax: +90 4642280025.

E-mail addresses: [dr.necati.kocyigit@gmail.com](mailto:dr.necati.kocyigit@gmail.com), [necati.kocyigit@erdogan.edu.tr](mailto:necati.kocyigit@erdogan.edu.tr) (N. Kocyigit).

<http://dx.doi.org/10.1016/j.ijrefrig.2014.05.027>

0140-7007/© 2014 Elsevier Ltd and IIR. All rights reserved.

Nomenclature		SV	solenoid valve
$COP_r$	coefficient of performance	VH	very high
$COP_{el}$	coefficient of performance based on electric power input	<i>Greek symbols</i>	
$\cos\phi$	power coefficient of compressor motor	$\epsilon$	pressure ratio
$h$	specific enthalpy of the refrigerant ( $\text{kJ kg}^{-1}$ )	$\eta_v$	volumetric efficiency of the compressor
$I$	current flow through the compressor and fans (A)	$\eta_s$	isentropic efficiency
$\dot{m}$	refrigerant mass flow rate ( $\text{kg s}^{-1}$ )	$\Delta$	increment
$n$	compressor motor speed (rpm)	<i>Subscripts</i>	
$v$	specific volume ( $\text{m}^3 \text{kg}^{-1}$ )	$a$	air
$\dot{Q}_c$	heat rejection rate at the condenser (W)	$c$	condenser
$\dot{Q}_e$	evaporator load (W)	$ca$	condensing absolute
$\dot{q}$	net cooling effect	$comp$	compressor
$P$	pressure (kPa)	$dis$	discharge
p-h	pressure-enthalpy	$e$	evaporator
$R$	residual values	$ea$	evaporation absolute
$T$	temperature ( $^{\circ}\text{C}$ )	$el$	electric
$U$	voltage across the heaters (V)	$exp$	expected values
$V_c$	compressor cylinder volume ( $\text{m}^3$ )	$f,e$	saturated liquid
$\dot{V}$	volume flow rate ( $\text{m}^3 \text{s}^{-1}$ )	$fg$	latent heat
$W_{el}$	electric motor power (W)	$g,e$	saturated vapor
<i>Abbreviation</i>		$max$	maximum values
AXV	automatic expansion valve	$min$	minimum values
EEV	electrical expansion valve	$nor$	normalized values
FDD	fault detection and diagnosis	$r$	refrigerant
H	high	$res$	residual values
L	low	$sat$	saturated
N	normal	$suc$	suction
No	no value	$sur$	surface of compressor
NCE	net cooling effect	$sc$	subcooling
VL	very low	$sh$	superheat
PH	partially high	$v$	specific volume
PL	partially low		

In the late 1980s, the earlier development of diagnostics of HVAC&R system operation was mainly performed by rule-based expert systems. During the late 1990s, the development of automating fault detection and diagnosis was emphasized. Inputs and outputs of an HVAC&R operating process can be mathematically related by using autoregressive models with exogenous inputs (ARX), artificial neural network (ANN) models, and many other developing models (Wang, 2001). Both ARX and ANN are called black-box because they require less physical knowledge of the operating process. These technologies are expected to be commercially available after laboratory and field tests.

The key to successful troubleshooting is the knowledge of how a refrigerating system operates and how each component functions in the system. Because a refrigeration system has at least four components connected by tubing, the effect of the operation of each component on the other three ones must be understood. A problem in one component may cause malfunctions in others. Knowledge of refrigeration theory and the operation of the components are necessary for successful troubleshooting. Besides component failures, external factors can also cause refrigeration system problems. These factors include water quality, air quality, and power supply.

Operating procedures and weather conditions can have an effect on the system. Load changes may cause further problems. One or more of these conditions may occur at any given time. Therefore, it is vital that we have an overall knowledge of system performance (Dossat, 1991).

In the past, methods for fault detection, diagnostics, and prognostics (FDD) were applied to various systems, such as vapor compression refrigeration systems (Tassou and Grace, 2005) and direct expansion cooling equipment (Li and Braun, 2007). Other publications of research have been presented on FDD itself (Han et al., 2011; Piacentino and Talamo, 2013).

In general, current FDD algorithms for vapor compression cycles are divided into two categories: steady-state model-based algorithms and neural network/fuzzy model approaches (Halm-Owoo and Suen, 2002). The characterization of vapor compression system faults has been pursued by many investigators. Rossi and Braun (1997) developed a technique that uses only temperature measurements to detect and diagnose five commonly occurring faults in rooftop air-conditioning systems. Breuker and Braun (1998) tested the sensitivity of the FDD method in a laboratory setting. The rooftop air conditioning unit was operated in a simulated building using typical on-off control over a range of operating

conditions and fault levels. Grimmelius et al. (1995) developed an on-line failure diagnosis system for a vapor compression refrigeration system used in a naval vessel or a refrigerated plant. Stylianou and Nikanpour (1996) provided a performance monitoring, fault detection and diagnosis of reciprocating chillers. Kim and Kim (2005) tested a water-to-water heat pump system with a variable speed compressor and an electrical expansion valve (EEV). They also provided an FDD algorithm along with two different rule-based charts depending on the compressor status. Proctor (2006) markets an expert system within a database that uses technician gathered system information to diagnose system faults.

Faults can be divided into two categories: 1) *hard* failures that occur abruptly and either cause the system to stop functioning or not meet comfort conditions and 2) *soft* faults that cause degradation in performance but allow continued operation of the system. The techniques that have been developed for diagnosing soft faults in vapor compression cooling equipment can be described in terms of a series of steps described by Isermann (1984). The first step is fault detection, in which a fault is indicated when the performance of a monitored system has deviated from expectation. The second step, diagnosis, determines which malfunctioning component is causing the fault. Following diagnosis, fault evaluation assesses the impact of the fault on system performance. Finally, a decision is made on how to react to the fault. Expert knowledge could be used to set larger thresholds that would guarantee that the detected faults are important and should be repaired (Braun, 2003).

Several investigators have proposed the use of thermodynamic impact to diagnose faults. They considered a packaged air conditioner with a fixed orifice as the expansion device, a reciprocating compressor with on/off control, fixed condenser and evaporator air flows, and R22 as the refrigerant. Isermann (1984) emphasized that condenser fouling is equivalent to having a smaller condenser and leads to higher condensing temperatures and pressures than the normal (no fault) case. Braun (2003) illustrated that the condenser fouling and low refrigerant can be distinguished by their unique effects on thermodynamic measurements. Bulgurcu (2009) released a book on maintenance, troubleshooting and service process in HVAC&R systems. Although significant progress has been made in this field, the number of faults that can be effectively diagnosed is still very limited.

Based on previous review, we found a gap between the information required to apply a general theory of diagnosis and the limited information of the p-h diagram. In this study, we conduct the fault diagnosis of a vapor compression refrigeration system applying hermetic reciprocating compressor through a proposed new method. The method is based on cycle analysis to put theoretical information of FDD and the limited information of the p-h diagram together. The proposed approach has much more diagnostic ability. The major objective of the present research is to test a basic vapor compression refrigeration experimental setup in order to map system parameters during fault-free and imposed-fault operations. System operating conditions are monitored, and performance parameters are recorded. Eight faults are imposed and investigated with the proposed method: (i) compressor failure, (ii) compressor valve leakage, (iii) restricted filter-drier, (iv) restricted automatic

expansion valve, (v) refrigerant undercharge, (vi) refrigerant overcharge, (vii) dirty condenser, (viii) evaporator fan failure. These collected results are used for the development of the new fault detection and diagnosis (FDD) method.

## 2. Fault detection and diagnosis

To analyze the performance of the refrigeration system, four points (1, 2, 3, and 4) on the p-h diagram (Fig. 1) and their measured and calculated values such as temperatures of points 1, 2, 3, and 4 ( $T_1$ ,  $T_2$ ,  $T_3$ , and  $T_4$ ) high side pressure ( $P_c$ ) and low side pressure ( $P_e$ ), refrigerants mass flow rate ( $\dot{m}$ ), current ( $I$ ), voltage ( $U$ ), and cosine  $\phi$  are required.

The differences between the actually measured values of an operating parameter, such as temperature  $T$  ( $^{\circ}\text{C}$ ), pressure  $P$  (Pa), volume flow rate  $\dot{V}$  ( $\text{m}^3\text{s}^{-1}$ ) or mass flow rate  $\dot{m}$  ( $\text{kgs}^{-1}$ ) and the expected values (estimated, simulated, or set points) of temperature  $T_{\text{exp}}$ , pressure  $P_{\text{exp}}$ , volume flow rate  $\dot{V}_{\text{exp}}$ , or mass flow rate  $\dot{m}_{\text{exp}}$  under normal operating conditions are called *residual*. A fault can be detected by investigating and analyzing residuals (Wang, 2001).

A temperature residual  $T_{\text{res}}$  ( $^{\circ}\text{C}$ ), a pressure residual  $P_{\text{res}}$  (Pa), or a volume flow rate residual  $\dot{V}_{\text{res}}$  ( $\text{m}^3\text{s}^{-1}$ ) can be calculated from

$$T_{\text{res}} = T - T_{\text{exp}} \quad (1)$$

$$P_{\text{res}} = P - P_{\text{exp}} \quad (2)$$

$$\dot{V}_{\text{res}} = \dot{V} - \dot{V}_{\text{exp}} \quad (3)$$

where, the subscript exp indicates expected (predicted) values and the units of  $T_{\text{exp}}$ ,  $P_{\text{exp}}$ , and  $\dot{V}_{\text{exp}}$  are the same as those of  $T$ ,  $P$ , and  $\dot{V}$ . Most of the measured operating parameters in a fault detection and diagnostic system are the same monitored

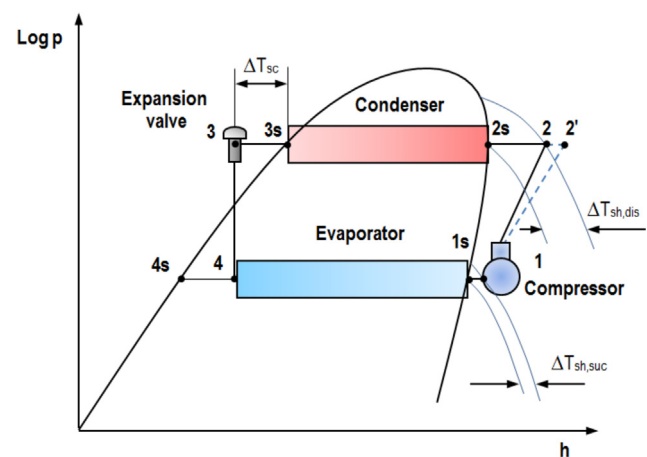


**Fig. 1 – Points of meaningful instrument readings in refrigeration cycle on the p-h diagram. ( $\Delta T_{\text{sh,suc}}$ : suction superheat,  $\Delta T_{\text{sh,dis}}$ : discharge superheat,  $\Delta T_{\text{sc}}$ : subcooling, point 1s: saturated vapor point of point 1, point 1: suction, point 2: discharge, point 2s: saturated vapor point of point 2, point 2': discharge with entropy increase, point 3s: saturated liquid of point 3, point 3: sub-cooled liquid at the expansion valve, point 4s: saturated liquid of point 4, point 4: evaporator input).**

parameters (sensed or measured) as in an energy management and control system (EMCS).

Residuals are often normalized so that the dominant symptom may have approximately the same magnitude for different types of faults. The residual  $R$  can be normalized as

$$R_{\text{nor}} = \frac{R - R_{\text{min}}}{R_{\text{max}} - R_{\text{min}}} \quad (4)$$

where  $R_{\text{nor}}$  is the normalized residual while  $R_{\text{max}}$  and  $R_{\text{min}}$  are maximum and minimum residuals, respectively.

A simple analysis of a standard vapor compression refrigeration system can be carried out by assuming a) steady flow, b) negligible kinetic and potential energy changes across each component, and c) no heat transfer in connecting pipe lines. The steady flow energy equation is applied to each of the four components.

### 2.1. Evaporator

Heat transfer rate at evaporator or refrigeration capacity  $\dot{Q}_e$  is given by:

$$\dot{Q}_e = \dot{m}(h_1 - h_4) \quad (5)$$

where  $\dot{m}$  is the refrigerant mass flow rate in  $\text{kg s}^{-1}$ ,  $h_1$  and  $h_4$  are specific enthalpies at the exit and inlet to the evaporator respectively.

### 2.2. Compressor

Power input to the compressor,  $\dot{W}_c$  is given by:

$$\dot{W}_c = \dot{m}(h_2 - h_1) \quad (6)$$

where  $h_2$  and  $h_1$  are specific enthalpies at the exit and inlet to the compressor respectively.

At any point in the cycle, the mass flow rate of refrigerant  $\dot{m}$  can be written in terms of volumetric flow rate and specific volume. By applying the mass flow rate equation to the inlet condition of the compressor,

$$\dot{m} = \frac{\dot{V}_1}{v_1} \quad (7)$$

where  $\dot{V}_1$  is the volumetric flow rate at compressor inlet and  $v_1$  is the specific volume at compressor inlet.

The compression ratio is given by:

$$\varepsilon = \frac{P_c}{P_e} \quad (8)$$

where  $P_c$  is the absolute condensing pressure and  $P_e$  is the absolute evaporating pressure.

Volumetric efficiency of compressor is given by:

$$\eta_v = \frac{\dot{m}_r v_1}{V_c n / 60} \quad (9)$$

where  $V_c$  is cylinder volume of compressor and  $n$  is the compressor speed.

Isentropic efficiency of the compressor is defined as:

$$\eta_s = \frac{\dot{W}_s}{\dot{W}_c} \quad (10)$$

where  $\dot{W}_s$  is the isentropic work of compressor.

### 2.3. Condenser

Heat transfer rate at the condenser,  $\dot{Q}_c$  is given by:

$$\dot{Q}_c = \dot{m}_r(h_2 - h_3) \quad (11)$$

where  $h_2$  and  $h_3$  are specific enthalpies at the inlet and exit to the condenser respectively.

### 2.4. Expansion device

During the throttling process in the expansion valve, it is assumed that there is no heat transfer to the environment, and it was mentioned earlier that the changes in kinetic and potential energies are negligible. Therefore, we have the following expression:

$$h_3 = h_4 \quad (12)$$

The exit condition of the expansion device lies in the two-phase region. One can write:

$$h_4 = (1 - x_4)h_{f,e} + x_4h_{g,e} = h_f + x_4h_{fg} \quad (13)$$

where  $x_4$  is the quality of the refrigerant at point 4, while  $h_{f,e}$ ,  $h_{g,e}$  and  $h_{fg}$  are saturated liquid enthalpy, saturated vapor enthalpy and latent heat of vaporization at the evaporator pressure, respectively.

The ratio of the evaporator load to the compressor power gives the coefficient of performance for the refrigeration system:

$$\text{COP} = \frac{\dot{Q}_e}{\dot{W}_c} \quad (14)$$

On the other hand, the coefficient of performance based on electric power input can be determined from the ratio of the evaporator load to the electric power consumption of the overall system:

$$\text{COP}_{\text{el}} = \frac{\dot{Q}_e}{\dot{W}_{\text{el}}} \quad (15)$$

where  $\dot{W}_{\text{el}}$  is the sum of electric power inputs to the motors of compressor, fans of the condenser and the evaporator.

Some terminologies on the p-h diagram (Fig. 1.) are explained as followings:

The suction superheat can be calculated by

$$\Delta T_{\text{sh,suc}} = T_1 - T_{1s} \quad (16)$$

where  $T_1$  is the suction temperature at point 1 and  $T_{1s}$  is the saturated vapor temperature of point 1.

The discharge superheat can be calculated by

$$\Delta T_{\text{sh,dis}} = T_2 - T_{2s} \quad (17)$$

where  $T_2$  is the discharge temperature and  $T_{2s}$  is the saturated vapor temperature of point 2.

The subcooling can be calculated by

$$\Delta T_{\text{sc}} = T_{3s} - T_3 \quad (18)$$

where  $T_3$  is the liquid temperature at the inlet of expansion valve and  $T_{3s}$  is the saturated liquid temperature of point 3.

The net cooling effect (NCE) can be calculated by

$$\Delta h_{1-4} = \dot{q} = h_1 - h_4 \quad (19)$$

where  $h_1$  is the specific enthalpy at point 1 and  $h_4$  is the specific enthalpy at point 4.

The vapor compression refrigeration cycle has four main components which are the compressor, the condenser, expansion device, and the evaporator (Fig. 1). Each main component is connected to each other by installing pipes which are called as the line. The refrigerant flows through each component by means of lines. The inlet to the compressor is called *suction line*. It brings the low pressure vapor into the compressor. The suction line connects the evaporator outlet (point 1s) and the compressor inlet (point 1). After the compressor compresses the refrigerant into a high pressure vapor, it removes it to the outlet called *discharge line*. The discharge line connects the compressor outlet (point 2) and the condenser inlet (point 2s). This occurs (in theory) at a constant entropy. On the other hand, the compression process occurs at constant entropy only in the ideal cycle. In the real world, entropy will increase during the compression process, resulting in even higher discharge temperatures and adding the amount of heat to the refrigerant. Thus, the compressor outlet is represented by point 2'. After the condenser changes the high pressure refrigerant from a high temperature vapor to a low temperature and high pressure liquid refrigerant, it leaves the condenser through a line called *liquid line*. The liquid line connects the condenser outlet (point 3s) and the expansion valve inlet (point 3). The high pressure refrigerant then flows through a filter drier to the automatic expansion valve (AXV) which meters the correct amount of liquid refrigerant into the evaporator. As AXV meters the refrigerant, the high pressure liquid changes to a low pressure, low temperature, and saturated liquid/vapor. The saturated liquid/vapor enters the evaporator and is changed to a low pressure, dry vapor. The low pressure, dry vapor is then returned to the compressor in the suction line. Thus, the cycle then starts over. The saturation temperature can be defined as the temperature of a liquid or vapor, where if any heat is added or removed, a change of state takes place.

### 3. Description of the experimental setup

The refrigeration troubleshooting experimental setup (Bulgurcu, 2010) consists of a hermetic reciprocating compressor, a finned type air cooled condenser, an automatic expansion valve and a unit type evaporator, as shown in Fig. 2. The system was charged with 600 g of R134a.

The compressor has a swept volume of  $7.95 \text{ cm}^3 \text{ rev}^{-1}$  and it has an average speed of 2800 rpm. The air-cooled condenser has a heat transfer area of  $0.075 \text{ m}^2$ . The evaporator was made from copper tube with finned aluminum. The refrigeration load was provided to the evaporator by the heat transferred from surrounding air.

The constant pressure expansion valve is operated by evaporator or valve-outlet pressure. It regulates the mass flow of the liquid refrigerant entering the evaporator and maintains this pressure at a constant value (ASHRAE, 2006).

As shown in Fig. 2, the refrigeration experimental setup has a compressor delivering the refrigerant to the condenser. A fan blows air over the condenser. The refrigerant passes

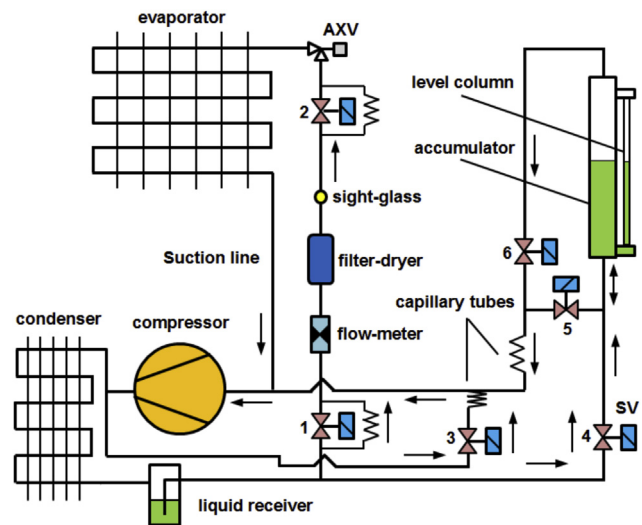


Fig. 2 – Schematic diagram of basic refrigeration experimental setup. (AXV: Automatic expansion valve, SV: Solenoid valve).

through the solenoid valve (1), filter-drier, sight glass, second solenoid valve (2), an expansion device, and then goes to the evaporator. Another fan blows air over the evaporator. The refrigerant returns to the compressor through the suction line. The liquid refrigerant passes through the solenoid valve (4), and then enters the accumulator. The accumulator is connected to the refrigeration system by top (for vapor refrigerant) and bottom side (for liquid refrigerant). It has a column indicating the refrigerant level. When the solenoid valve (5) or (6) is opened, the refrigerant is added to the system. When the solenoid valve (3) is opened, the refrigerant bypasses the suction line.

All temperature measurements were performed using PTC type thermistors. The temperatures of the experimental setup at the inlet and outlet of the cooling components were also measured using thermocouples in direct contact with the refrigerant. The refrigerant mass flow rate passing through the liquid line was continuously monitored by a turbine type flow meter.

### 4. Experiments

For better understanding of these faults on the troubleshooting set, it is necessary to know the p-h diagram of normal operating conditions. Experiments have been made in the air conditioned laboratory maintained at  $25 \text{ }^\circ\text{C}$  ambient temperature, and the evaporator is also placed in the same ambient conditions. Thus, its operating temperatures are higher than those in winter conditions.

Eight faulty conditions cause the refrigeration cycle were plotted differently on the p-h diagram and were named as shown in Table 1.

Each fault mode was performed and explained respectively as below:



**Table 1 – Description of studied faults, abbreviations, and determination of level of fault.**

Faults	Abbreviations	Determination of level of fault during test
Compressor failure-doesn't work	CDW	compressor switch off
Restricted filter-drier	RFD	% of normal pressure drop through AXV
Restricted automatic expansion valve	RXV	% of normal pressure drop through evaporator
Compressor valve leakage	CVL	% of refrigerant flow rate
Refrigerant undercharge	RU	% undercharge from the correct charge
Refrigerant overcharge	RO	% overcharge from the correct charge
Dirty condenser	DC	% of air flow rate reduction
Evaporator fan failure	EFF	evaporator fan switch off
Normal condition	NC	fault free test

- 1) CDW: If the compressor is switched off, the compressor will not work. In this case, the evaporating pressure is nearly the same as the condensing pressure. Thus, both of them are represented by a straight line, as shown in Fig. 4(a).
- 2) RFD: When the normally open solenoid valve 1 (SV<sub>1</sub>) closes, simulation of the restricted filter-drier fault (RFD) occurs. In this case, while refrigerant starts to flow through the filter from bypass capillary tube instead of liquid line, sweating on the filter-drier occurs. During this case, the mass flow rate of refrigerant decreases and both the suction line and the discharge line pressures decrease, as shown in Fig. 4(b).
- 3) RXV: When the normally open solenoid valve 2 (SV<sub>2</sub>) closes, simulation of the restricted automatic expansion valve (AXV) fault (RXV) occurs. In this case, while refrigerant starts to flow through the filter from bypass capillary tube instead of liquid line, sweating on the expansion valve occurs. During this case, the mass flow rate of refrigerant decreases and both the suction line and the discharge line pressures decrease, as shown in Fig. 4(c).
- 4) CVL: Compressor valve leakage can be caused by worn cylinder surfaces and piston rings as well as a clogged valve plate. The suction line and the discharge line are connected by the normally closed valve (SV<sub>3</sub>). When SV<sub>3</sub> opens, simulation of the compressor valve leakage fault (CVL) occurs. In this case, the hot gas will return from the liquid line to the suction line bypass valve (3). Thus, refrigerant mass flow rate decreases in the refrigeration system, as shown in Fig. 4(d).
- 5) RU: Both the solenoid valve 4 (SV<sub>4</sub>) and the solenoid valve 6 (SV<sub>6</sub>) are the normally closed valve. If both SV<sub>4</sub> and SV<sub>6</sub> open, the liquid refrigerant and the gaseous refrigerant are easily displaced and the liquid refrigerant is accumulated in the accumulator. It is required to close valves as soon as the liquid refrigerant reaching the highest level of the sight glass tube. In this case, simulation of the undercharged refrigerant (RU) occurs. Thus, the refrigeration system will have lack of refrigerant to perform the cooling process, as shown in Fig. 4(e).
- 6) RO: When the normally closed solenoid valve 5 (SV<sub>5</sub>) or valve (SV<sub>6</sub>) open, simulation of the overcharged refrigerant fault (RO) occurs. In this case, the liquid refrigerant flows through the capillary tube from the accumulator to the suction line and thus, the refrigerant charge of the system increases. It is required to close valves as soon as the liquid refrigerant observing at the lower level of the sight glass tube, as shown in Fig. 4(f).
- 7) DC: The dirty condenser (DC) is simulated by restricting the air mass flow rate of fan while the condenser is clogged by paper (leaves, paper pieces, dust, etc.). Thus, DC occurs. In this case, the heat transfer capacity of the condenser will decrease. Eighty percent of failures are caused by fully or partially blocking of the finned frontal area of the condenser, as shown in Fig. 4(g).
- 8) EFF: If the evaporator fan motor switched off, the heat transfer coefficient of the evaporator will decrease. Thus, simulation of the evaporator fan motor fault (EFF) occurs. The refrigerant does not evaporate in the evaporator, and then it flows through the suction line to the compressor in the liquid phase, as shown in Fig. 4(h).

Calculated values are expressed as a percentage, and NC values (fault free) are considered to be 100% after collecting data from the refrigeration system. Experimental data collected from the experimental setup are listed in Table 2. Changes in percentage of calculated results with respect to normal condition are listed in Table 3. Each difference in

**Table 2 – Experimental data.**

Measurements	P <sub>e</sub> [kPa]	P <sub>c</sub> [kPa]	T <sub>1</sub> [°C]	T <sub>2</sub> [°C]	T <sub>3</sub> [°C]	T <sub>4</sub> [°C]	T <sub>sur</sub> [°C]	$\dot{m}$ [gs <sup>-1</sup> ]	I [A]	U [volt]	cos $\phi$
Faults											
CDW	560	560	25	25	25	25	25	0	0	0	0
RFD	210	980	14.5	61.5	37.6	1.6	40	3.0	2.1	225	0.79
RXV	190	950	16.3	61.2	37.1	-0.2	40.7	2.7	2.07	226	0.78
CVL	280	860	10	63.3	34.5	7.6	41.5	2.9	2.13	225	0.80
RU	190	860	20.1	62.5	34.1	-0.2	41	2.5	2.04	225	0.77
RO	256	1090	6.2	50.5	40.3	5.7	32	2.6	2.19	226	0.81
DC	230	1300	17.1	70.4	48.9	3.6	42	3.6	2.19	224	0.82
EFF	195	840	0.5	46.5	33.8	0.5	24.4	3.4	2.08	226	0.77
NC	225	990	10	59	38.3	3.2	38.5	3.9	2.14	227	0.79

**Table 3 – Change of calculated results based on normal condition (%).**

Measurements	$T_{sh}$	$T_{sc}$	$\dot{Q}_e$	$\dot{Q}_c$	$\dot{Q}_{comp}$	$W_{el}$	$\eta_v$	$\eta_s$	COP	$COP_{el}$	$\epsilon$
Faults											
CDW	0	0	0	0	0	0	0	0	0	0	1
RFD	189	109	80	79	74	97	84	113	108	82	105
RXV	242	95	73	71	63	94	82	124	115	77	109
CVL	35	164	76	79	90	100	63	69	85	77	83
RU	299	173	71	69	60	91	78	124	118	77	110
RO	07	130	64	62	52	105	60	124	122	61	99
DC	199	82	86	88	94	106	94	121	91	83	126
EFF	0	77	87	83	65	94	93	124	133	92	95
NC	100	100	100	100	100	100	100	100	100	100	100

values shows the code of fault which characterizes the type of fault.

## 5. Results and discussion

This section will start with the discussion of the use of the p-h diagram for detection of the faults. Later, the performance of the proposed method will be demonstrated and discussed for each fault. Finally, the classification of the observed variables will be assigned the classification of symptom of failures for detection of the faults.

To use the p-h diagram, we suggest the following procedures:

First, thermodynamic properties would be calculated after the experimental data is collected.

Second, the CoolPack software (CoolPack, 2010) would prepare the refrigeration cycle on the p-h diagram given in Figs. 3 and 4 from the thermodynamic properties such as the temperature (T), the pressure (p), the entropy (s), and the enthalpy (h).

Third, we interpret the p-h lines to diagnose the faults. Under the normal conditions (NC), the cycle would stay within the boundaries indicated by the points marked as 1, 2, 3, and 4 in the diagram and the cycle is plotted with dashed line on the p-h diagram as shown in Fig. 3. However, when the system has a faulty condition, the refrigeration cycle would operate among the points marked as 1', 2', 3' and 4' and the cycle is plotted with continuous line on the p-h diagram as shown in Fig. 3. The cycle of normal conditions and faulty conditions are plotted with dash line and continuous line respectively so that both cycles can be compared with each other.

Let's consider the system had a DC fault cycle as shown in Fig 3 and the fragment of DC fault cycle as shown in Fig. 4(g). If the condenser is clogged by paper, the DC fault occurs. When the system had a DC fault, the refrigeration cycle would operate among faulty points. Fig. 3 has more details about thermodynamic properties of the refrigeration cycle. The fault could be identified after the deviation of each thermodynamic property was analyzed. All faulty conditions would create their unique changes at the p-h diagram.

Each fault mode is plotted with continuous lines on fragments of the refrigeration cycle with faults on the p-h diagram was compared with NC which was plotted with dash lines as shown in Fig. 4, respectively. The performance of the

proposed method would be demonstrated in Fig. 4 and discussed in terms of cycle for each fault as below:

Fig. 4(a) shows that CDW causes the refrigeration system to be  $P_c$  the same as  $P_e$ . The refrigeration cycle on the p-h diagram is represented by a straight line. The temperature of the refrigerant, which is a mixture of saturated liquid and vapor, is the same as the ambient temperature.

Fig. 4(b) shows that RFD causes the suction superheat and enthalpy ( $h_1$ ) to increase, the evaporating temperature ( $T_e$ ) and pressure ( $P_e$ ) to decrease, the degree of subcooling to increase slightly, and the condensing temperature and pressure ( $P_c$ ) to stay almost the same value or to increase indistinctly on the p-h diagram. Because of the additional expansion in the liquid line, refrigerant mass flow reduces, thereby decreasing the refrigeration capacity.

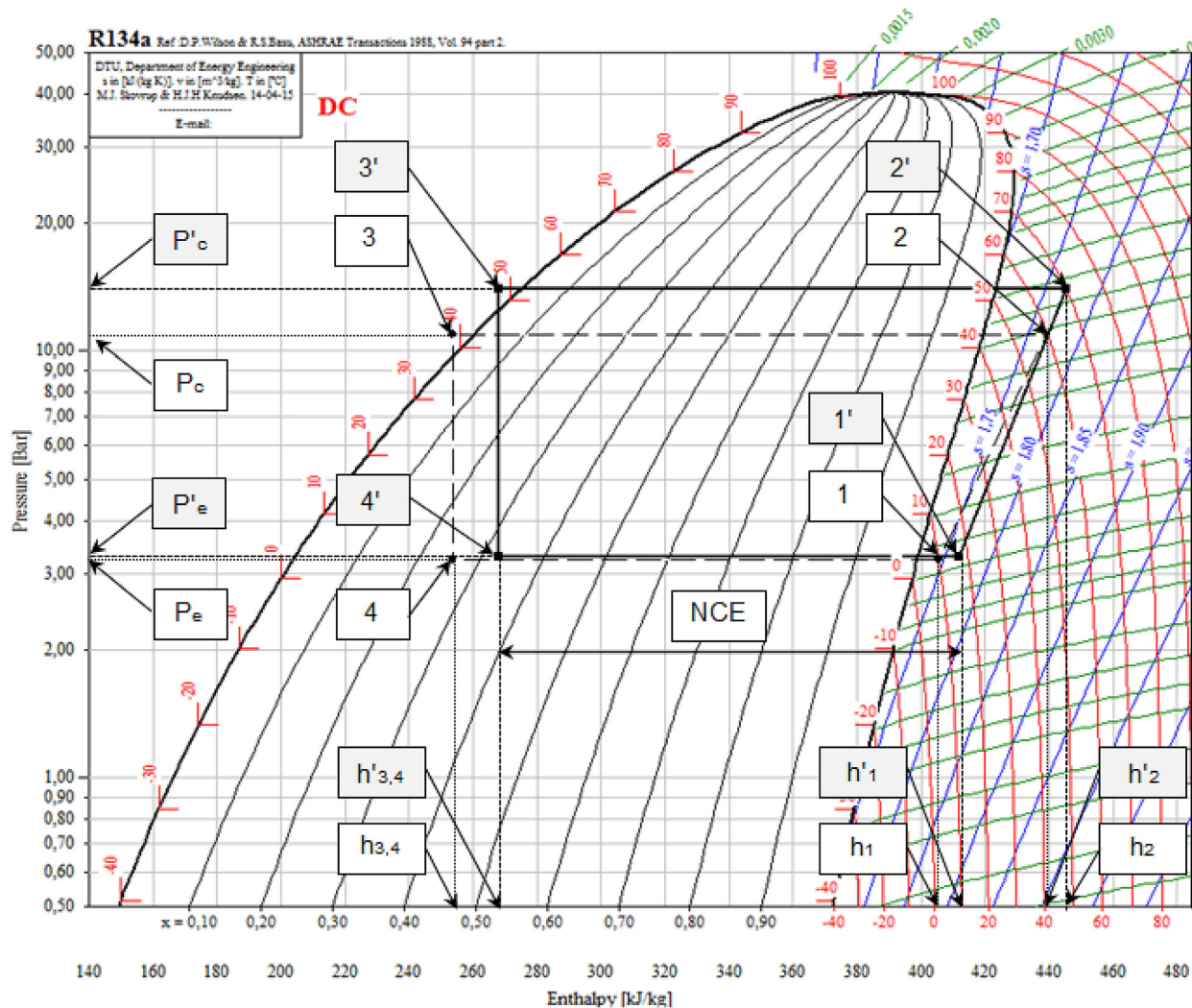
Fig. 4(c) shows that RXV causes the suction superheat and the enthalpy of point 1 ( $h_1$ ) to increase, the evaporating temperature and pressure ( $P_e$ ) to decrease, the condensing temperature and pressure ( $P_c$ ) to decrease slightly, subcooling and the enthalpy of point 3 ( $h_3$ ) to decrease, the refrigeration capacity to increase.

Fig. 4(d) shows that CVL causes the refrigerant mass flow rate to decrease in the refrigeration system. Thus,  $P_e$  indistinctly increases and  $P_c$  decreases rather, while the suction superheat and the enthalpy of point 1 ( $h_1$ ) rather decreases, the discharge superheat and the enthalpy of point 2 rather increases, and the subcooling slightly increases. On the other hand, the entropy increases rather. The refrigerant mass flow reduces, thus decreasing the refrigeration capacity.

Fig. 4(e) shows that RU causes the refrigerant charge of system to decrease. Thus,  $P_e$  indistinctly decreases and  $P_c$  slightly decreases and the superheating and the enthalpy of point 1 ( $h_1$ ) and 2 ( $h_2$ ) rather increase while the subcooling and the enthalpy of point 3 ( $h_3$ ) slightly increase. The refrigerant mass flow rate reduces, thus decreasing the refrigeration capacity.

Fig. 4(f) shows that RO causes both  $P_e$  and  $P_c$  to increase. But the suction superheat is zero and the enthalpy of point 1 ( $h_1$ ) slightly decreases. The subcooling and the enthalpy of point 3 ( $h_3$ ) slightly decrease. The refrigerant mass flow rate increases, but lack of net cooling effect occurs.

Fig. 4(g) shows that DC causes the heat transfer capacity of the condenser to decrease. In this faulty case, the high side pressure ( $P_c$ ) reasonably increase and the low side pressure ( $P_e$ ) increases slightly. The subcooling and the enthalpy of point 3 ( $h_3$ ) rather decrease but the suction superheat and the



**Fig. 3 – The p-h diagram of the refrigeration cycle with DC fault. (DC : Dirty Condenser,  $P_c$ : High pressure of NC,  $P'_c$ : High pressure of DC,  $P_e$ : High pressure of NC,  $P'_e$ : High pressure of DC,  $h_1$ : Enthalpy of point 1,  $h'_1$ : Enthalpy of point 1',  $h_2$ : Enthalpy of point 2,  $h'_2$ : Enthalpy of point 2',  $h_{3,4}$ : Enthalpy of point 3 and 4,  $h'_{3,4}$ : Enthalpy of point 3' and 4', NCE: Net Cooling Effect).**

enthalpy of point 1 ( $h_1$ ) rather increase. On the other hand the discharge superheat and the enthalpy of point 2 ( $h_2$ ) slightly increase.

Fig. 4(h) shows that EFF causes the heat transfer coefficient of the evaporator to decrease. The refrigerant does not evaporate sufficiently in the evaporator, and then it flows through the suction line to the compressor in the liquid phase. This condition is very detrimental for the compressor.  $P_e$  and  $P_c$  decrease, the superheating is nearly absent, but the subcooling rather increases. The enthalpy of point 1 ( $h_1$ ) and 2 ( $h_2$ ) decrease but the enthalpy of point 3 ( $h_3$ ) rather increases. The low pressure switch opens the control circuit. The refrigeration capacity decreases because of the ice layer.

The performance of the proposed method would be demonstrated on graphs as shown in Fig. 5 and discussed in terms of calculated values of cycles for each fault as below:

Fig. 5(a) shows the highest superheating occurs at RU fault, while the lowest occurs at RO and EFF fault conditions. The

heat efficiency of evaporator is reduced by increasing the suction superheat. Conversely, refrigerant back flow may occur by decreasing the superheat, which can cause a mechanical compressor failure. As shown in Fig. 5(a), the highest subcooling occurs at RU fault whereas the lowest occurs at RO and EFF faults conditions.

As shown in Fig. 5(b), the changes in the heat capacity of the evaporator, condenser, compressor, and the changes in the electrical input to the compressor as a function of the imposed fault have been investigated. It is seen that the lowest heat capacity values occur at RO condition and the heat capacity changes in the evaporator, condenser and compressor are parallel to each other. It is also seen that heat flow rates of condenser and compressor decrease whereas the electrical power input to the compressor increase in RO condition.

The changes of the efficiencies including isentropic and volumetric are depicted in Fig. 5(c). This figure shows that the



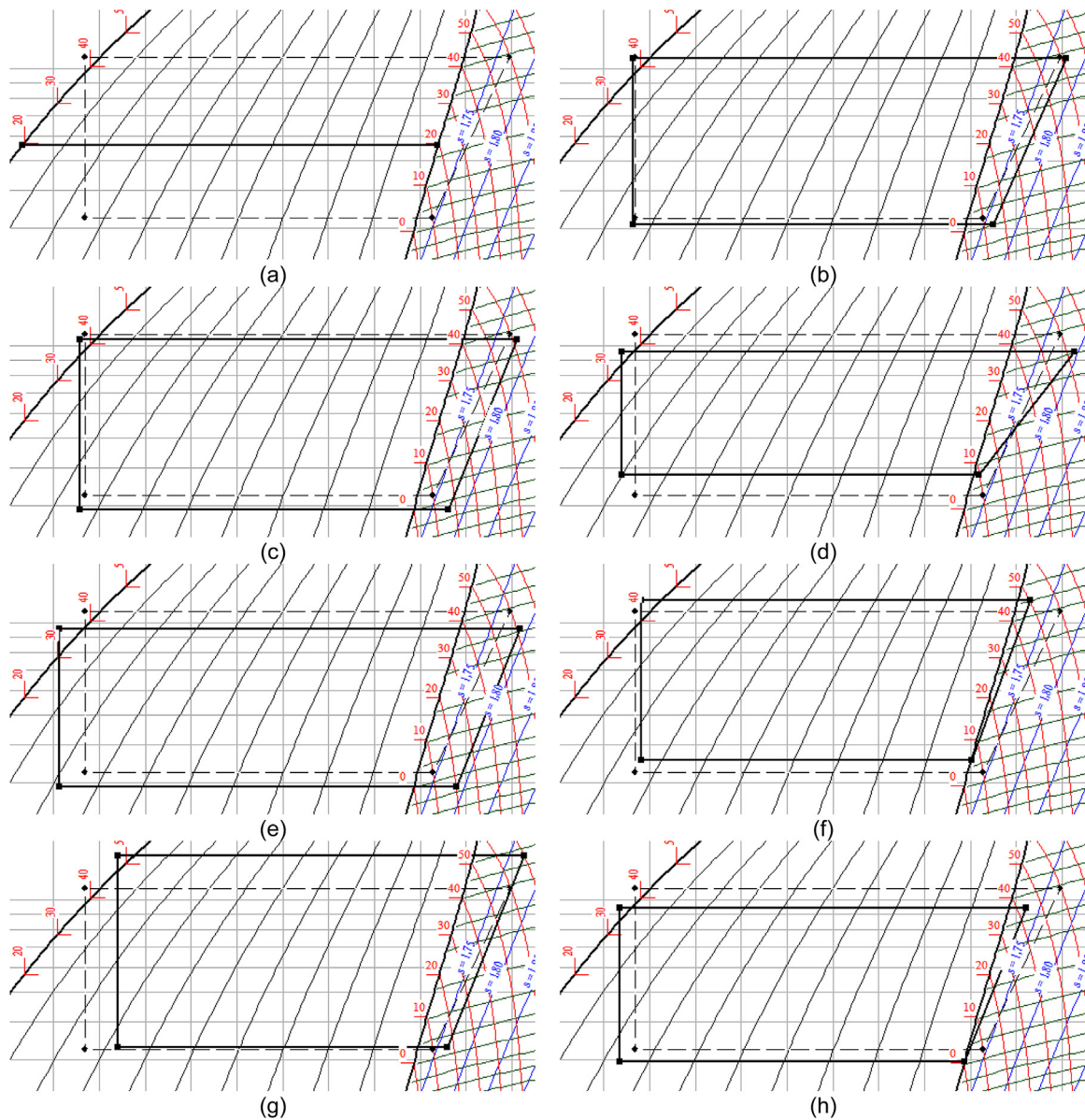


**Fig. 4 – Fragments of the refrigeration cycle with faults on the p-h diagram (a) CDW, (b) RFD, (c) RXV, (d) CVL, (e) RU, (g) RO, (h) EFF.**

maximum values of the efficiencies are obtained at EFF fault, while the minimum occurs at CVL.

As shown in Fig. 5(d), the changes in COP and  $COP_{el}$  are examined in FDR, RXV, CVL, and RU conditions. The value of  $COP_{el}$  is at the minimum level in the RO faulty condition, while the COP is just below the maximum value. Fig. 4(d) also depicts that the values of COP and  $COP_{el}$  in the DC and EFF faulty conditions are higher than NC.

Fig. 5(e) shows that pressure ratio of the compressor reaches a maximum value in the DC condition but it has a minimum value in the CVL condition.

According to Table 3, RFD faulty condition has the suction superheat is observed to be over 89% and that of over cooling appears 9% above NC. The values of capacity and volume is seen to be below whereas that of the isentropic outcome

appears 13% above the norm while COP exceeds NC by 8%,  $COP_{el}$  is observed to be 8% below NC. The pressure rate increases by 5%.

Table 3 also shows, in case of CVL faulty condition, the suction superheat drops against the expectations whereas the degree of subcooling rises in compliance with the predictions. The heat capacity of the condenser and evaporator seems to lower than the normal operation terms. The volume and isentropic efficiency are observed to be 37% and minimum 31% below NC. Likewise, the COP as well as the pressure rate is seen to be low.

In case of RU faulty condition, Table 3 shows that the suction superheat and the overcooling appear to be over NC (199% and 73% respectively), and the heat capacity rates fall below NC. While the volumetric efficiency falls 22% below

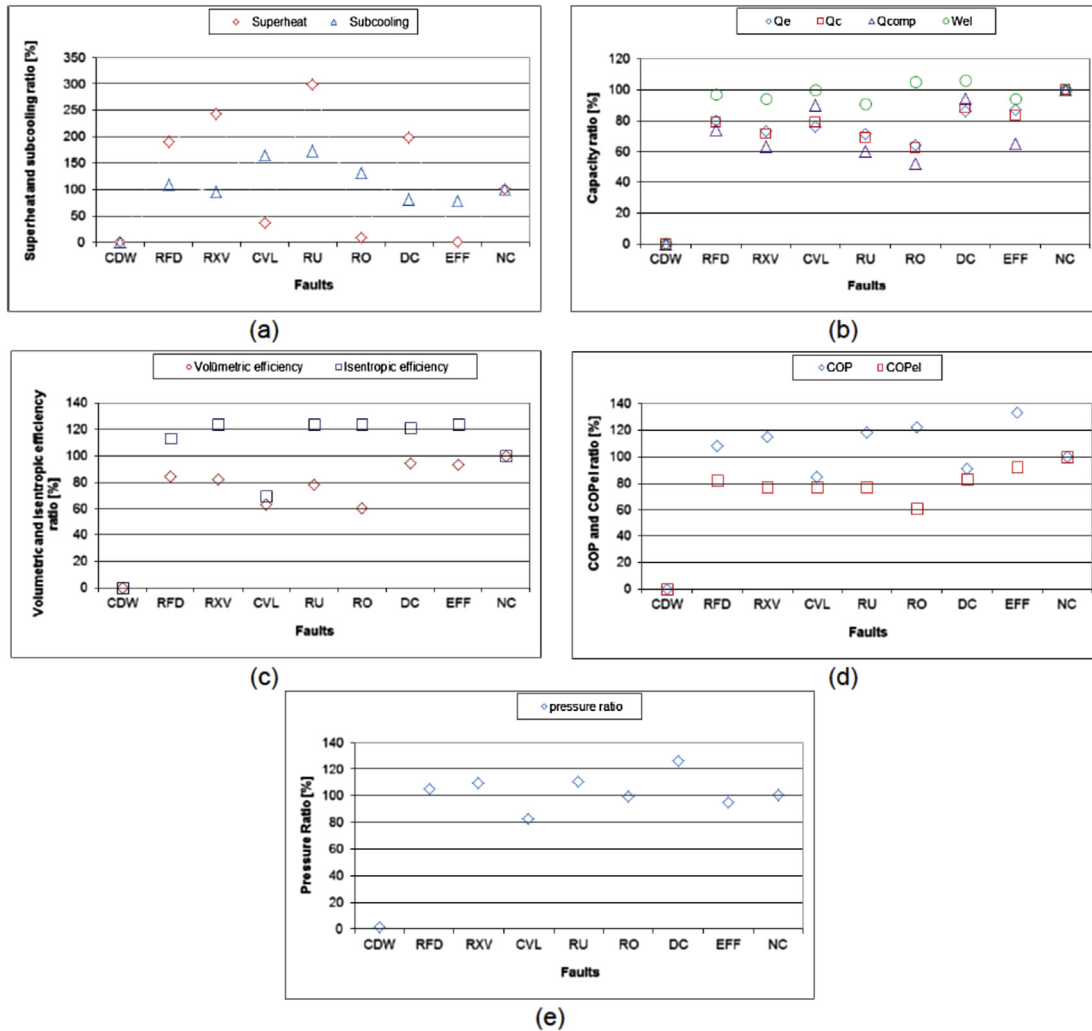


Fig. 5 – Graphs for different fault conditions. (a) Change degrees of superheating and subcooling ratio, (b) Change of evaporator, condenser and compressor capacities and electrical input to the compressor ratio, (c) Change of volumetric and isentropic efficiency ratio (d) Change of COP and COP<sub>el</sub> ratio, (e) Change of pressure ratio.

NC, the isentropic efficiency rises 24% above NC against the predictions. Likewise, while the COP<sub>el</sub> falls 33% below NC, the COP exceeds NC by 18% against the predictions. Besides, the pressure rate against the expectations gets 10% over NC.

When there is a fault with flow (refrigerant overcharge), the suction superheat gets lower than NC whereas the value of overheating exceeds NC. According to Table 3, the heat capacity rates of condenser and compressor get 36%, 38%, 48% lower than NC respectively. While the volumetric efficiency is

Table 4 – The classification of the observed variables.

Measurements	$P_e$		$P_c$		$T_{sh}$		$T_{sc}$		$\dot{m}$		$T_{sur}$	
	Assigned classification		Assigned classification		Assigned classification		Assigned classification		Assigned classification		Assigned classification	
	Min	Max	Min	Max	Min	Max	Min	Max	Min	Max	Min	Max
No	–	–	–	–	0	0.1	0	0.1	0	0.1	25	25.1
VL	190	195	560	830	0.1	2.0	0.1	3.0	0.1	2.5	25.1	30
L	195	200	830	930	2.0	4.0	3.0	3.5	2.5	3.0	30	34
PL	200	220	930	980	4.0	6.0	3.5	4.0	3.0	3.5	34	38
N	220	230	980	1020	6.0	8.0	4.0	4.5	3.5	4.0	38	40
PH	230	250	1020	1100	8.0	11.0	4.5	5.5	–	–	40	42
H	250	280	1100	1200	11.0	15.0	5.5	6.5	–	–	–	–
VH	280	560	1200	1300	15.0	21.0	6.5	7.5	–	–	–	–

**Table 5 – Symptoms of failure.**

Measurements Faults	$P_e$ [kPa]	$P_c$ [kPa]	$T_{sh}$ [K]	$T_{sc}$ [K]	$\dot{m}$ [gs <sup>-1</sup> ]	$T_{sur}$ [K]
CDW	VH	VL	No	No	No	No
RFD	PL	PL	H	PH	L	PH
RXV	VL	PL	VH	M	L	H
CVL	H	L	L	PL	L	PH
RU	VL	L	VH	VH	VL	PH
RO	H	PH	VL	H	L	L
DC	PH	VH	H	PH	PL	PH
EFF	L	VL	VL	L	PL	VL

seen to get 40% lower, the isentropic efficiency gets 24% higher than NC. Likewise, the COP and COP<sub>el</sub> display changes similar to those with the volumetric and isentropic efficiency. The pressure rate display the same level as NC.

In case of DC, Table 3 shows that the suction superheat gets 99% higher and the overheating gets 18% lower than NC. The heat capacity rates, except the electric motor, display lower values than NC. While the volumetric efficiency gets 6% lower, the isentropic efficiency gets 21% higher than NC. Likewise, the COP is seen to be 9% below NC, the COP<sub>el</sub> is displayed even 17% lower. The pressure rate, however, is observed to get 26% above NC.

Finally, for detection of the faults, the classification of the observed variables was required to assign the classification of symptom of failures. The assigned classifications and their values in minimum and maximum limits were determined and considered as N, PH, H, VH, PL, L, and VL in Table 4. The malfunctions of refrigeration system would be detected by using symptoms of failures listed in Table 5.

## 6. Conclusions

In this paper, we developed a vapor compression refrigeration system experimental setup to diagnose faults based on the p-h diagram. For this purpose, eight common fault scenarios were imposed on the refrigeration system, and results have been discussed in terms of possible faults in basic refrigeration systems.

Eight faults were easily observed to cause changes on the p-h diagram and in the performance parameters of the system. It was found that these changes varied depending on the type of expansion valve used, accessories, ambient temperature and fault level in the refrigeration system.

## REFERENCES

ASHRAE Handbook Refrigeration, 2006. American Society of Heating, Refrigerating and Air-Conditioning Engineers, Inc., 1791 Tullie Circle, N.E., Atlanta.

- Braun, J.E., 2003. Automated fault detection and diagnostics for vapor compression cooling equipment. *J. Sol. Energy Eng.* 125, 1–10.
- Breuker, M.S., Braun, J.E., 1998. Evaluating the performance of a fault detection and diagnostic system for vapor compression equipment. *Int. J. Heat. Vent. Air Cond. Refrig. Res.* 4, 401–425.
- Bulgurcu, H., 2009. Maintenance, Troubleshooting and Service Process in HVAC&R Systems. ISKAV Technical Book Series No: 5, Istanbul (printed in Turkish).
- Bulgurcu, H., 2010. S-804-Refrigeration Troubleshooting Demonstration Unit. Available at Url: <http://www.deneysan.com/products/S-804eng.pdf> (accessed 06.06.10.).
- CoolPack, 2010. A Collection of Simulation Tools for Refrigeration. Available at Url: [www.et.dtu.dk/CoolPack](http://www.et.dtu.dk/CoolPack) (accessed 16.06.13.).
- Dossat, R.J., 1991. Principles of Refrigeration. Prentice Hall, USA, New Jersey.
- Grimmelius, H.T., Woud, J.K., Been, G., 1995. On-line failure diagnosis for compression refrigeration plants. *Int. J. Refrigeration* 18, 31–41.
- Halm-Owoo, A.K., Suen, K.O., 2002. Applications of fault detection and diagnostic techniques for refrigeration and air conditioning: a review of basic principles. *Proc. Inst. Mech. Eng. Part J. Process Mech. Eng.* 216, 121–132.
- Han, H., Gua, B., Wanga, T., Li, Z.R., 2011. Important sensors for chiller fault detection and diagnosis (FDD) from the perspective of feature selection and machine learning. *Int. J. Refrigeration* 34, 586–599.
- Isermann, R., 1984. Process fault detection based on modeling and estimation—a survey. *Automatica* 20, 387–404.
- Kim, M., Kim, M.S., 2005. Performance investigation of a variable speed vapor compression system for fault detection and diagnosis. *Int. J. Refrigeration* 28, 481–488.
- Li, H., Braun, J.E., 2007. An overall performance index for characterizing the economic impact of faults in direct expansion cooling equipment. *Int. J. Refrigeration* 30, 299–310.
- McIntosh, I.B.D., Mitchell, J.W., Beckman, W.A., 2000. Fault detection and diagnosis in chillers – part I: model development and application. *ASHRAE Trans.* 106, 268–282.
- Piacentino, A., Talamo, M., 2013. Innovative thermoeconomic diagnosis of multiple faults in air conditioning units: methodological improvements and increased reliability of results. *Int. J. Refrigeration* 36, 2343–2365.
- Proctor, J., 2006. CheckMe!™ Expert Analysis System Developed by Proctor Engineering Group, 418 Mission Avenue, San Rafael, CA 94901, Available at Url: <http://www.proctoreng.com/checkme/checkme.html> (accessed 05.11.06.).
- Rossi, T.M., Braun, J.E., 1997. A statistical, rule-based fault detection and diagnostic method for vapor compression air conditioners. *Int. J. Heat. Vent. Air Cond. Refrig. Res.* 3, 19–37.
- Stylianou, M., Nikanpour, D., 1996. Performance monitoring, fault detection and diagnosis of reciprocating chillers. *ASHRAE Trans.* 102, 615–627.
- Tassou, S.A., Grace, I.N., 2005. Fault diagnosis and refrigerant leak detection in vapor compression refrigeration systems. *Int. J. Refrigeration* 28, 680–688.
- Wang, S.K., 2001. Handbook of Air Conditioning and Refrigeration, second ed. McGraw-Hill, New York. Available at Url: <http://www.gmpua.com/CleanRoom/HVAC/Cooling/HandbookofAirConditioningandRefrigeration.pdf>. (accessed 30.12.13.).